Quaternary Science Reviews 300 (2023) 107883

Contents lists available at ScienceDirect

Quaternary Science Reviews

journal homepage: www.elsevier.com/locate/quascirev

Environmental and climate evolution in the Southwest USA since the last interglacial deduced from the pollen record from Stoneman lake, Arizona

Gonzalo Jiménez-Moreno [a, *], R. Scott Anderson [b], Vera Markgraf [b], Spencer E. Staley [c], Peter J. Fawcett [c]

[a] Departamento de Estratigrafía y Paleontología, Universidad de Granada, 18002, Granada, Spain
[b] Environmental Programs, School of Earth & Sustainability, Northern Arizona University, Flagstaff, AZ, 86011, USA
[c] Department of Earth and Planetary Sciences, University of New Mexico, Albuquerque, NM, 87131, USA

ARTICLE INFO

Article history:
Received 16 September 2022
Received in revised form
9 November 2022
Accepted 19 November 2022
Available online 30 November 2022

ABSTRACT

Long and continuous lake sedimentary records offer enormous potential for interpreting the paleoenvironmental histories of the past and for understanding how terrestrial environments might adapt in the context of current global warming. However, sedimentary records that contain multiple glacial-interglacial cycles are scarce in continental basins. An ~80 m sediment core was recently obtained from Stoneman Lake (STL), Arizona, containing a unique record of the last ~1.3 Ma. Here we show a detailed pollen study of the topmost ~10 m of the record, covering the last climatic cycle since the Last Interglacial period (MIS5-MIS1; last ~130,000 years = 130 kyr), with the goal of broadening our knowledge of the paleoenvironmental history of the arid North American Southwest in the past. The STL pollen record shows that the MIS5e interglacial was the warmest period of the last 130 kyr. This is deduced by the abundance of pollen types from plants that today exist at lower elevations that occurred around the STL at that time. These include *Pinus edulis* and other associated low elevation thermophilous plants such as *Juniperus*, *Ambrosia*, Amaranthaceae, Asteraceae and *Artemisia*. Climate cooled rapidly and dramatically at the MIS5-4 boundary, which triggered a displacement of forest species towards lower elevation, causing *P. ponderosa* to occupy the study area. MIS3 was characterized by relatively warmer climate conditions with 3 prominent climatic oscillations (MIS3a, b and c). The coldest conditions were reached during MIS2 (LGM), when a ~1000 m displacement towards lower elevations of the subalpine forest species relative to present is observed. This is deduced by the highest abundance of *Picea* (~20 −25%) and *Abies* in the STL record, indicating their occurrence in the study area. Warming during the last deglaciation is evidenced by a shift of vegetation towards higher altitudes and the development of a montane forest composed mainly of *Pinus ponderosa* and *Quercus* replacing the LGM subalpine species. This montane forest remained abundant throughout the Holocene. This study shows that orbital-scale climate changes (mainly precession and eccentricity changes) forced vegetation and lake-level oscillations, documenting that insolation had a main role in controlling environmental change in this area. Climate projections of enhanced warming predict that *P. edulis* and *Juniperus* forest species will occupy the study area in the near future.

1. Introduction

One of the great challenges facing humanity today is a rapidly changing climate and its impact on the environment, economy and society (IPCC, 2022). The latest forecastsfrom the Intergovernmental Panel on Climate Change (IPCC, 2022) suggest that the possible ~2 °C increase in temperatures by the end of the 21st century, relative to the period from 1850 to 1900, will affect atmospheric dynamics and cause an increase in average annual evaporation. In this respect, considerable increases in the occurrence of exceptionally hot seasons in North America in the 21st-century are also anticipated (Diffenbaugh and Giorgi, 2012).

* Corresponding author.
E-mail address: gonzaloj@ugr.es (G. Jiménez-Moreno).

https://doi.org/10.1016/j.quascirev.2022.107883

Climate models also project decreases in winter precipitation over the southwestern USA (Seager and Vecchi, 2010), which will lead to tree die-offs and increased prevalence of catastrophic wildfires in mountain areas (Alizadeh et al., 2021; IPCC, 2022), much of which is already occurring. Enhanced drought, land use changes, and growth in the water-demanding human population are generating stress on environments and societies in that region (Seager et al., 2007; Karl et al., 2009; Cayan et al., 2010; MacDonald, 2010; Williams et al., 2013). An important question then arises: how will ecosystems respond to climate change in southwestern North America? Answering this question requires detailed paleoecological and paleoclimatic studies to help us understand the relationship between climate and the environment in the past, especially during warmer and drier periods than at present such as MIS 5e.

The Last Interglacial period (LIG), commonly called the "Eemian" (or "Sangamonian" in the USA) in terrestrial environments and corresponding to the global marine isotope stage MIS5e, was a period of significantly higher temperatures than the present interglacial in many parts of the Northern Hemisphere and similar to some projections of temperatures for the next century (Otto-Bliesner et al., 2013; Capron et al., 2017). Terrestrial summer temperatures in the Northern Hemisphere were particularly elevated with estimated surface temperature anomalies between 2 and 5 °C above the preindustrial level (Otto-Bliesner et al., 2013). The LIG was also characterized by higher global sea level and reduced ice sheet extent relative to the Holocene, consistent with the IPCC's predictions for responses to future global warming. This period also witnessed atmospheric CO_2 levels of up to 300 ppm, similar to the pre-industrial era (Brovkin et al., 2016). All these characteristics make the LIG a key period as a natural analog for future environmental scenarios due to global warming and/or drought increase (Yin and Berger, 2015). The LIG offers many advantages for comparison with the present and the Holocene; the continental configuration, flora and fauna were almost identical to the current ones and being a recent period, sedimentary records are well preserved, providing us with excellent paleoenvironmental records at high resolution.

In 2014 two long sedimentary cores, STL14-1A and 1B, were obtained from Stoneman Lake, Arizona (Fig. 1). The correlation of the lithological and physical properties of cores A and B permitted a composite reconstruction of the sedimentary sequence of this lake (Staley et al., 2022). Based on a suite of AMS radiocarbon dates in the upper 6 m of the record, as well as four tephras dating to the mid-Pleistocene Transition, the sedimentary sequence likely contains a continuous record of the last ~1.3 Ma (Staley et al., 2022). Here we show a high-resolution palynological and charcoal study of the topmost ~10 m of the STL14 record, covering the last climatic cycle since the LIG (last 130 kyr; Fig. 2). STL is located just above the lower elevation limit of the montane *Pinus ponderosa* forest and the ecotone with the *P. edulis* (piñon)-*Juniperus* (juniper) woodland (Fig. 1). Therefore, the pollen stratigraphy from STL should be very sensitive to changes in the composition and elevation of these forest communities through time, which are predominantly dependent on climate (Fall 1997).

Our pollen and charcoal data, together with the previously reported chronological age control and sedimentological data provide insights about the paleoenvironmental and climate history of arid southwestern North America and allow us to understand how terrestrial environments might adapt in the future to global warming (Williams et al., 2013; IPCC, 2022). In addition, results from this study will improve our knowledge about the natural climatic and environmental dynamics of the current interglacial in the absence of anthropogenic forcing and the degree of alteration of natural vegetation trends in the region due to human impact in the past millennia. Further, the comparison of the STL-14 record with other long and detailed paleoclimatic records from the western USA and globally allows us to obtain information on potential climatic triggers for past environmental change.

2. Study site

STL (34° 46′ 41"N, 111° 31′ 05"W, 2048 m above sea level) is located in central Arizona (Fig. 1) on the southwestern edge of the Colorado Plateau - the Mogollon Rim - and has a catchment area of 3.5 km^2. Basin bedrock is composed of basalts of the Mormon Mountain volcanic field of Middle Miocene to Late Pliocene age (Holm et al., 1989), which overlie Paleozoic limestones. STL is likely a sinkhole formed from the dissolution and collapse of these limestones (Dohm, 1995), although its origin could also be related to the collapse of an evacuated magma chamber (McCabe, 1971).

Historic data document that STL lake levels are sensitive to climate, having reached a maximum depth of ~5 m in 1980, and were generally high during the late 1970s to early 1990s (Malcolm Pirnie and ADEQ, 2000), a period of higher-than-average precipitation in the study area (Hereford, 2007). Lake levels have since declined steeply, and STL is currently a palustrine environment due to a prolonged early twenty-first century drought (Staudenmaier et al., 2014) and is seasonally dry during summer and fall (Fig. 1).

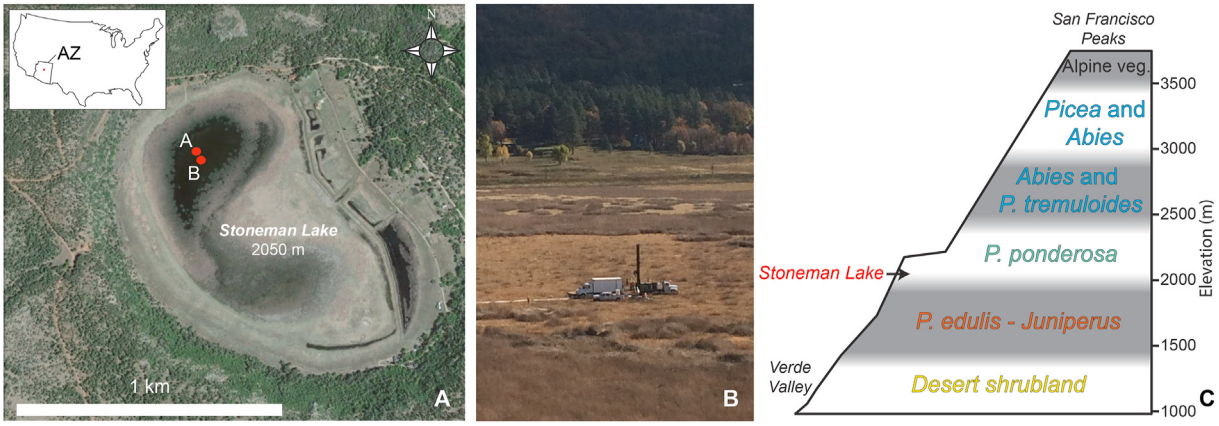

Fig. 1. Location (A), coring (B) and vegetation background of Stoneman Lake, Arizona (C). Photo of coring of STL-14 in October 2014. The distribution of plant communities by elevation in central Arizona is after Brown and Lowe (1982). Stoneman Lake is situated just above the ecotone between Ponderosa Pine (*Pinus ponderosa*) and Piñon (*P. edulis*) - Juniper (*Juniperus*) forests (C).

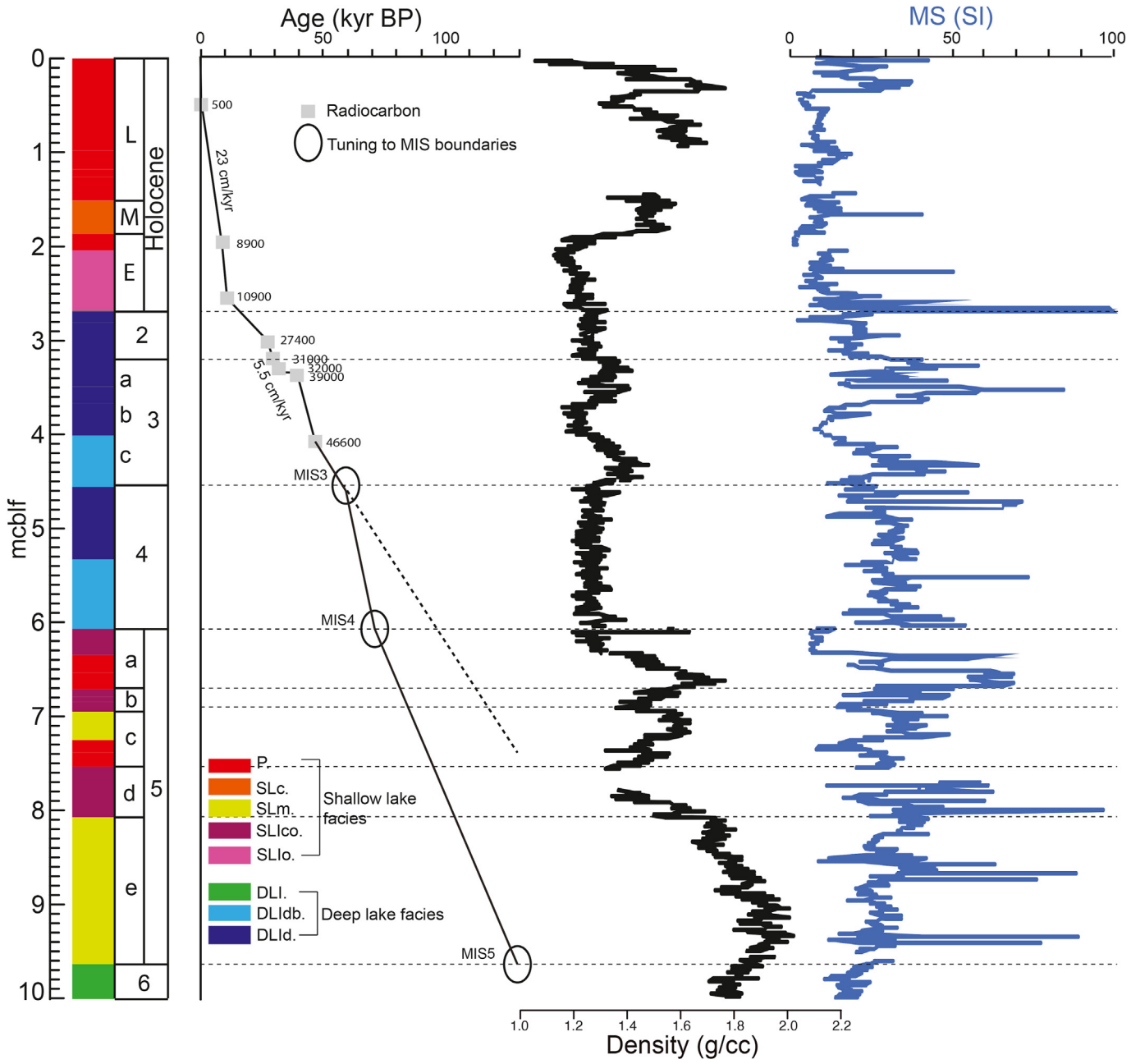

Fig. 2. Lithology, age model, density and magnetic susceptibility (MS) for composite core STL14. On the left are numerical dates for the radiocarbon analyses done on the upper part of the record. Suggested boundaries for MIS are marked by horizontal dashed lines. Our STL14 record was tuned to the LR04 isotopic record, and boundaries between MIS6-5 (130 kyr), 5–4 (71 kyr) and 4–3 (57 kyr) come from Lisiecki and Raymo (2005). Sedimentary facies characterization, density and MS data come from Staley et al. (2022). Lithofacies indicating shallow lacustrine conditions are: P: Banded clay-silt with common carbonaceous organic matter. SLc: Massive to banded clay-silt with common authigenic calcite. SLm: Massive clay-silt. SLlo: Interbedded couplets of organics and clay-silt. SLlco: Laminated to bedded organic-rich clay-silt with authigenic calcite laminae. Lithofacies indicating deep lacustrine conditions are: DLl: Laminated to thin-bedded clay-silt with occasional diatoms. DLldb: Bioturbated laminated to thin-bedded and banded clay-silt with common diatoms. DLld: Laminated to thin-bedded clay-silt and laminated diatomaceous ooze with common to dominant diatoms.

In the last decade, STL lake levels have not exceeded 50 cm (personal observations). Fluvial water inputs into the lake are negligible due to the small catchment area and modern lake levels are sustained by ground-water input, snowmelt from the immediate slopes around the lake, and ephemeral runoff events.

Climatic data for STL are not available directly. However, data from the nearby Happy Jack Ranger Station (2280 m asl; ~10.7 km ESE of STL; https://wrcc.dri.edu/cgi-bin/cliMAIN.pl?az3828) document a mean annual temperature of 7 °C, mean summer temperature of 14.8 °C and mean winter temperature of −0.8 °C. Precipitation in the study area is biseasonal, influenced both by Pacific frontal winter precipitation related to El Nino-Southern Oscillation (ENSO) (Cayan et al., 1999) and the North American summer monsoon (Metcalfe et al., 2015). Mean annual precipitation is 664.5 mm, with 45% occurring during winter (December–March) and 31% during summer (July–September).

STL is located near the lower elevational limit of the Sierran montane conifer forest, and the upper limit of the pygmy conifer forest (Brown and Lowe, 1978) (Fig. 1). *Pinus ponderosa* (ponderosa pine) is the dominant tree species in the former, with additional

tree species found around STL including *Cupressus arizonica* (Arizona cypress), *Quercus gambelii* (Gambel's oak), *Juniperus monosperma* (one-seed juniper), and *Juglans major* (Arizona walnut) (Hasbargen, 1994). The pygmy conifer forest occurring below STL (the ecotone is located at ~2050 masl in the study area), is dominated by *Pinus edulis* (Colorado pinon) and several junipers (*Juniperus monosperma*, *Juniperus deppeana*, *Juniperus osteosperma*), intermixed with drought-tolerant shrubs locally called a piñon-juniper woodland. At higher elevations above the Sierran montane conifer forest in the San Francisco Peaks, ~70 km to the north of STL, *Pseudotsuga menziesii* (Douglas fir), *Abies concolor* and *A. lasiocarpa* (white and subalpine fir), *Populus tremuloides* (quaking aspen) and *Picea englemannii* (Englemann spruce) occur together with other high-elevation species (Fig. 1).

3. Materials and methods

The STL14 composite sedimentary record was recovered in October 2014 using a truck-mounted coring device. Two cores, STL14-A and STL14-B were taken 30 m apart in the northern depocenter of STL (Fig. 1). STL14-A extended to the base of the lacustrine sequence and ended when further penetration was refused by basaltic rocks at 70.1 m below lake floor (mblf). STL14-B reached 30.1 mblf. Overall, 98% recovery was accomplished in the two cores. The cores were split and imaged at the Continental Scientific Drilling (CSD) facility at the University of Minnesota. Cores were scanned automatically by instrumentation mounted on multisensor core loggers producing 0.5-cm-resolution data sets that included different physical properties such as wet bulk density (by gamma attenuation) and magnetic susceptibility (Bartington MS2E point sensor) (Staley et al., 2022, Fig. 2). A composite core was constructed by correlating lithologic and physical properties of cores A and B in their overlapping section (see Staley et al., 2022 for details). Lithologic description and sedimentological analysis were previously carried out by Staley et al. (2022) (Fig. 2). Staley et al. (2022) studied the lithofacies of the STL14 sedimentary record and noticed a correlation with wet bulk density and bulk magnetic susceptibility (MS). In addition, they observed a correlation of middle and late Pleistocene glacial maxima to deep lake deposits defined by well-preserved bedding, increased biosilica, boreal pollen taxa (i.e., *Picea*), and lower density and MS. Interglacial periods were interpreted as associated with shallow-water deposits characterized by banded-to-massive siliciclastic material, some authigenic calcite, the alga *Phacotus*, and higher density and MS.

To develop an age model for the STL composite sediment core, we used radiocarbon analyses from the topmost part of the record (age dates going back to ~45 ka) and visual correlation between the STL14 facies-density record and the LR04 global mean benthic isotope stack (Lisiecki and Raymo, 2005), which features a well-established chronology (Table 1; Fig. 2; see Staley et al., 2022 for more details on the age-depth model). Well-dated tephras, including the Lava Creek B and the Bishop Ash, constrain age-depth relationships deeper in the core than this study, but are consistent with the radiocarbon age model (see Staley et al., 2022).

The STL14 cores were sampled for palynological analysis every 5–10 cm, depending on the sedimentary rate changes in the different sections of the core, throughout the upper 10 m of the record, which contains a sedimentary record of the last ~130 kyr based on the age model described above (Fig. 2). A total of 132 samples of two cubic centimeters (2 cc) were collected. Following the previously published age-depth model (Staley et al., 2022), the average age resolution between samples corresponds to ~1000 years. The pollen extraction method followed a modified Faegri and Iversen (1989) method. The sediment samples were processed with HCl (35%) and HF (70%) to remove the carbonates and silicates, respectively, from the sediment and concentrate the organic matter, and KOH (10%) to remove the cellulose fraction from the organic matter. The samples were sieved using a 10 μm nylon sieve to remove particles smaller than the pollen grains. Samples were then treated by acetolysis (H_2SO_4 and glacial acetic acid) to eliminate the rest of the unwanted organic matter in the samples. The residual material, together with glycerin, was mounted on microscope slides. Counting and identification of palynomorphs was carried out with a transmitted light microscope at 400x magnifications. Pollen grains are relatively abundant in the samples, and a number of terrestrial pollen grains between 200 and 306 were classified, enough to make environmental interpretations (Sánchez Goñi et al., 2002; Djamali and Cilleros, 2020). Pollen atlases, such as Beug (1961) and pollen reference material of plants that occur in the American SW were used for certain identifications. *Pinus* pollen

Table 1
Chronological control of the studied section of core STL14 (from Staley et al., 2022).

STL14 radiocarbon chronology[a]			
Sample	Core depth (mcblf)	Radiocarbon Age[b] (yrs)	Median calibrated age[c] (yrs)
STL14-1B-1C-1-45	0.45	427 ± 30	494
STL14-1B-2C-1-62	1.99	8026 ± 35	8887
STL14-1A-3C-1-63	2.55	9618 ± 37	10,943
STL14-1B-3C-1-7	3.01	23,104 ± 113	27,379
STL14-1B-3C-1-37	3.31	26,932 ± 156	31,092
STL14-1A-3C-1-142	3.34	28,211 ± 143	32,241
STL14-1B-3C-1-41	3.35	34,500 ± 253	39,649
STL14-1B-3C-1-114	4.08	43,390 ± 534	45,749
STL14-1A-4C-1-145	5.93	Radiocarbon not detected	> ~50,000
STL14-1B-5C-129	7.34	Radiocarbon not detected	> ~50,000
MIS boundary	**Core depth (mcblf)**	**Age[d] (ka)**	**Basis**
MIS 2 > 1	2.69	14	Facies change (shallowing); Radiocarbon
MIS 3 > 2	3.345	34 (29)	Radiocarbon dates
MIS 4 > 3	4.54	57	Facies change (shallowing)
MIS 5 > 4	6.06	72 (71)	Facies change (deepening)
MIS 6 > 5	9.63	132 (130)	Facies change (shallowing)

[a] ^{14}C-AMS dates of wood and aquatic vegetation macrofossils.
[b] With 1σ uncertainty.
[c] Using IntCal20 model of Reimer et al. (2020).
[d] MIS boundaries first described by Lisiecki and Raymo (2005) (in parenthesis) are redefined by Railsback et al. (2015).

was divided into two categories: *Pinus* indeterminate [most-likely including diploxylon (*P. ponderosa* or *P. contorta*) and haploxylon (*P. aristata*, *P. flexilis*)] and *P. edulis* (piñon). *P. edulis* pollen was differentiated from the rest of *Pinus* indeterminate pollen by its small size (generally smaller than 65 μm in breadth) and the presence of verrucae on the leptoma (Hansen and Cushing, 1973; Jacobs, 1985).

Pollen percentages have been calculated with respect to the total sum of terrestrial pollen excluding aquatic taxa (*Typha*, Cyperaceae, *Myriophyllum*, *Potamogeton* and *Nuphar*) in each analyzed sample. The most representative pollen types with occurrences higher than 1% are shown in Fig. 3. The percentages of algae (*Botryococcus, Pediastrum, Spirogyra* and *Zygnema*), *Isoetes* microspores and other non-pollen palynomorphs ("Non-Pollen Palynomorphs"; NPP such as *Filinia longiseta* eggs, oocytes of the aquatic flatworm *Neorhabdocoela* or mycorrhizal fungus *Glomus*) have been calculated with respect to the total sum of terrestrial pollen and are shown in Fig. 4. The pollen ratio of *Artemisia* versus *Picea* [A/P ratio = (A-P)/(A + P)] has been used in previous studies to determine changes in vegetation related to climate (for example, Toney and Anderson, 2006; Jiménez-Moreno et al., 2011, 2019; Johnson et al., 2013) and was also calculated in this study. Cluster analyses of the pollen and NPP data were done using the program CONISS (Grimm, 1987) (Figs. 3 and 4), with the goal of visualizing sets of samples with similar pollen assemblages.

We applied a Principal Components Analysis (PCA) to our pollen and NPP percentage data (Fig. 5). PCA locates variables (components) that represent, as much as possible, the variance of the multivariate data (Hammer et al., 2001). These new components are linear combinations of the original variables. The PCA can be used to reduce data sets to only two variables (the first two components), in order to summarize the data for comparison in graphs. PCA has been carried out using the Past4 software (Hammer et al., 2001).

Charcoal particles larger than 30 μm were counted in the palynological slides. Charcoal particles of large size between 60 and 100 μm were annotated (Fig. 4). Charcoal concentration (charcoal particles/cm^3) was calculated using the *Lycopodium* tracer concentration, in the same manner as the calculations for pollen concentration (Fig. 4).

4. Results

The forest pollen taxa that characterize the STL14 record are dominated by *Pinus* species, most likely including *P. ponderosa* (that grows in the area at present) and *P. edulis*, and in less abundance by the mixed and subalpine conifers *Picea* and *Abies*, and the thermophilous taxa *Quercus* and *Juniperus*. Regarding the herbaceous and shrubby taxa, pollen assemblages are dominated by *Artemisia*, Asteraceae, *Ambrosia*, Amaranthaceae, Poaceae and in smaller proportions, other shrubs such as *Ephedra* and *Sarcobatus* (Fig. 3). With respect to the NPPs, algal remains, such as *Pediastrum*, *Botryococcus, Spirogyra* and *Zygnema*, are abundant. Spores of *Isoetes* (Pteridophyta), mycorrhizal fungi such as *Glomus* and eggs of the rotifer *Filinia longiseta* also occur (Fig. 4).

The results of the PCA analysis on the main terrestrial pollen data (tPCA) show two primary groups of distinctive taxa (Fig. 5A and B). The tPC1 explains 45% of the variance and tPC2 explains 23% of the variance. One group (tPC1+) is characterized by a positive correlation with PC1 and is composed mainly of *Pinus* indet., *Picea*, *Abies*, *Pseudotsuga*, Poaceae and *Quercus*. The other group (tPC1-) is characterized by a negative correlation with PC1 and is mainly formed by *P. edulis*, *Artemisia*, *Ambrosia*, Amaranthaceae, Asteraceae, *Juniperus*, *Sarcobatus* and *Ephedra*.

The PCA applied to the NPP (Fig. 5C and D) shows that the nPC1 and nPC2 explain 57% and 24% of the variance, respectively. Two main groups of taxa are identified with this analysis: an nPC1+ group formed by *Pediastrum*, *Isoetes*, *Filinia longiseta* and *Botryococcus* and an nPC1- group made up of *Zygnema*, *Spirogyra*, *Debarya*, *Neorhabdocoela* and *Glomus*. The pollen data, summarized with the terrestrial pollen *P. edulis* + *Juniperus* abundance and A/P pollen ratio and NPP nPC1, change through time. Objective zonation of the pollen data by CONISS cluster analysis and visual examination allow a subdivision of the palynological record in vegetation into climatically distinct periods that roughly agree with the Marine Isotope Stages (MIS) identified for the last 130 kyr (Figs. 3 and 4; Lisiecki and Raymo, 2005; Cronin, 2010). In the sections below, we discuss the STL vegetation and climatic reconstructions for each of the identified MISs.

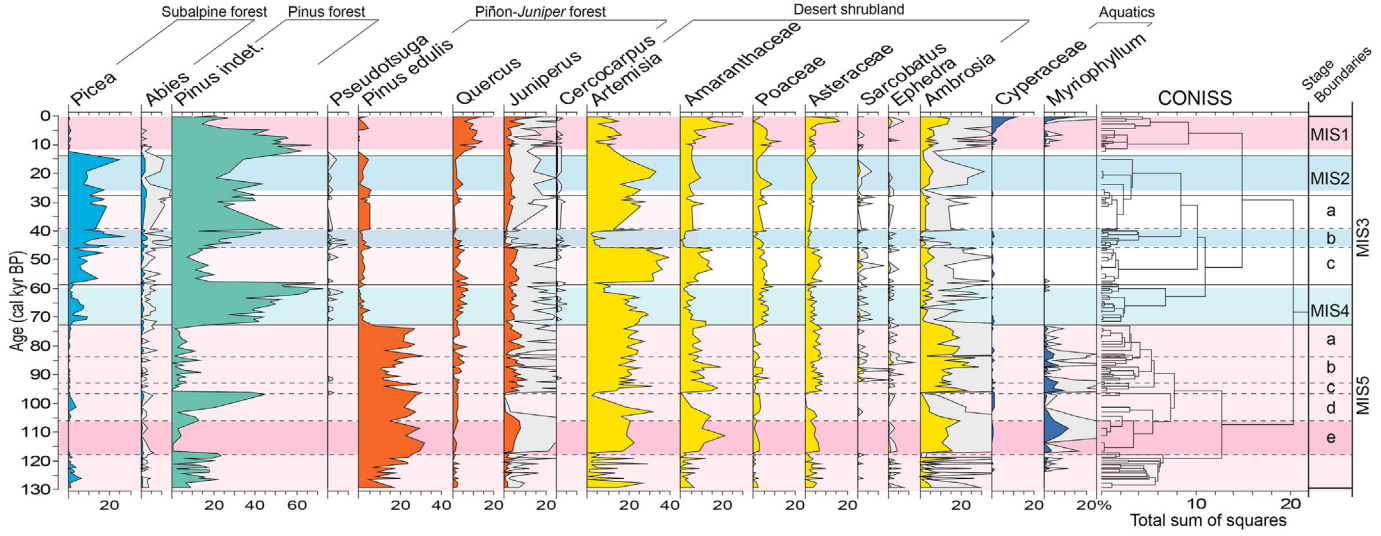

Fig. 3. Detailed pollen diagram of the STL14 record. Only taxa with abundances higher than 1% are shown. On the right are the cluster analysis done by CONISS (Grimm, 1987) and the MIS stage boundaries inferred from the visual comparison of pollen curves and the Lisiecki and Raymo (2005) record. Red and blue shading highlights the warm and cold phases recorded at STL.

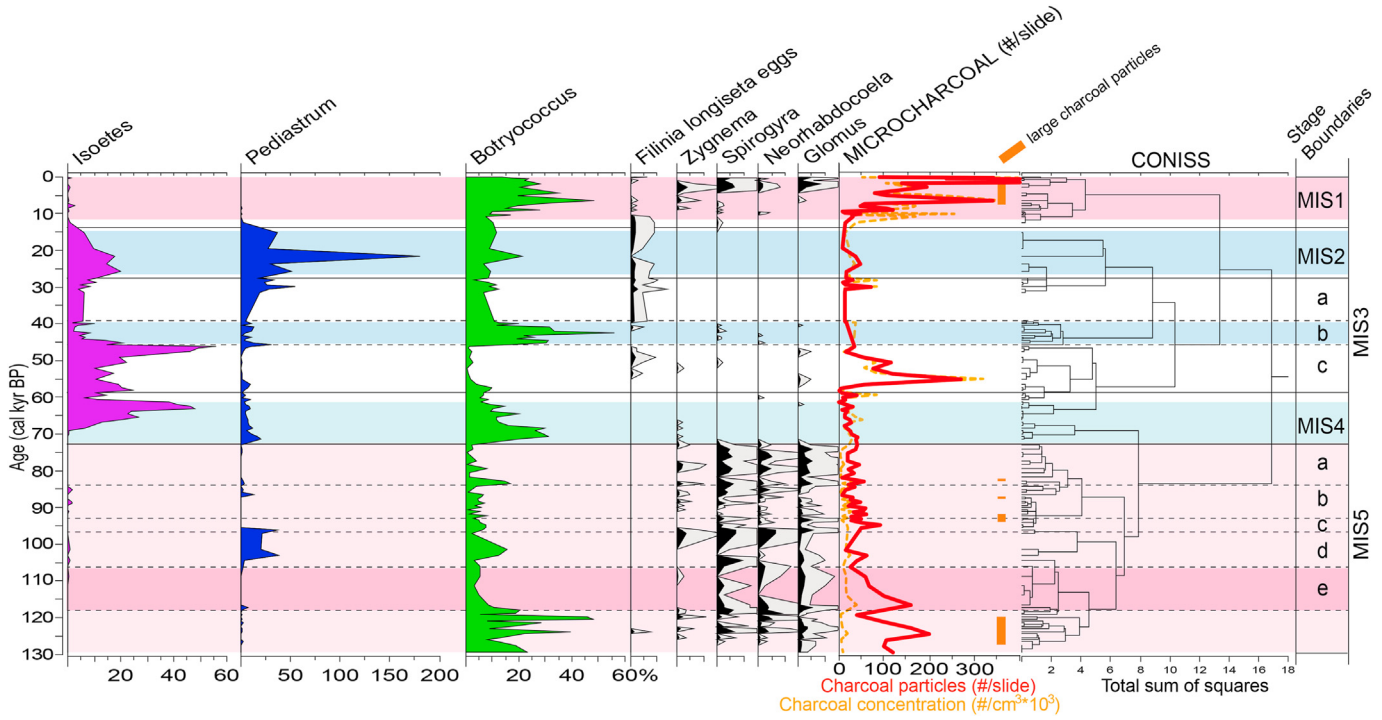

Fig. 4. Detailed Non Pollen Palynomorphs (NPP) and charcoal data from the STL14 record. The occurrence of large charcoal particles between 60 and 100 μm is indicated by orange rectangles. On the right are the cluster analysis done by CONISS (Grimm, 1987) and the MIS stage boundaries suggested by the pollen. Red and blue shading highlights the warm and cold phases recorded at STL.

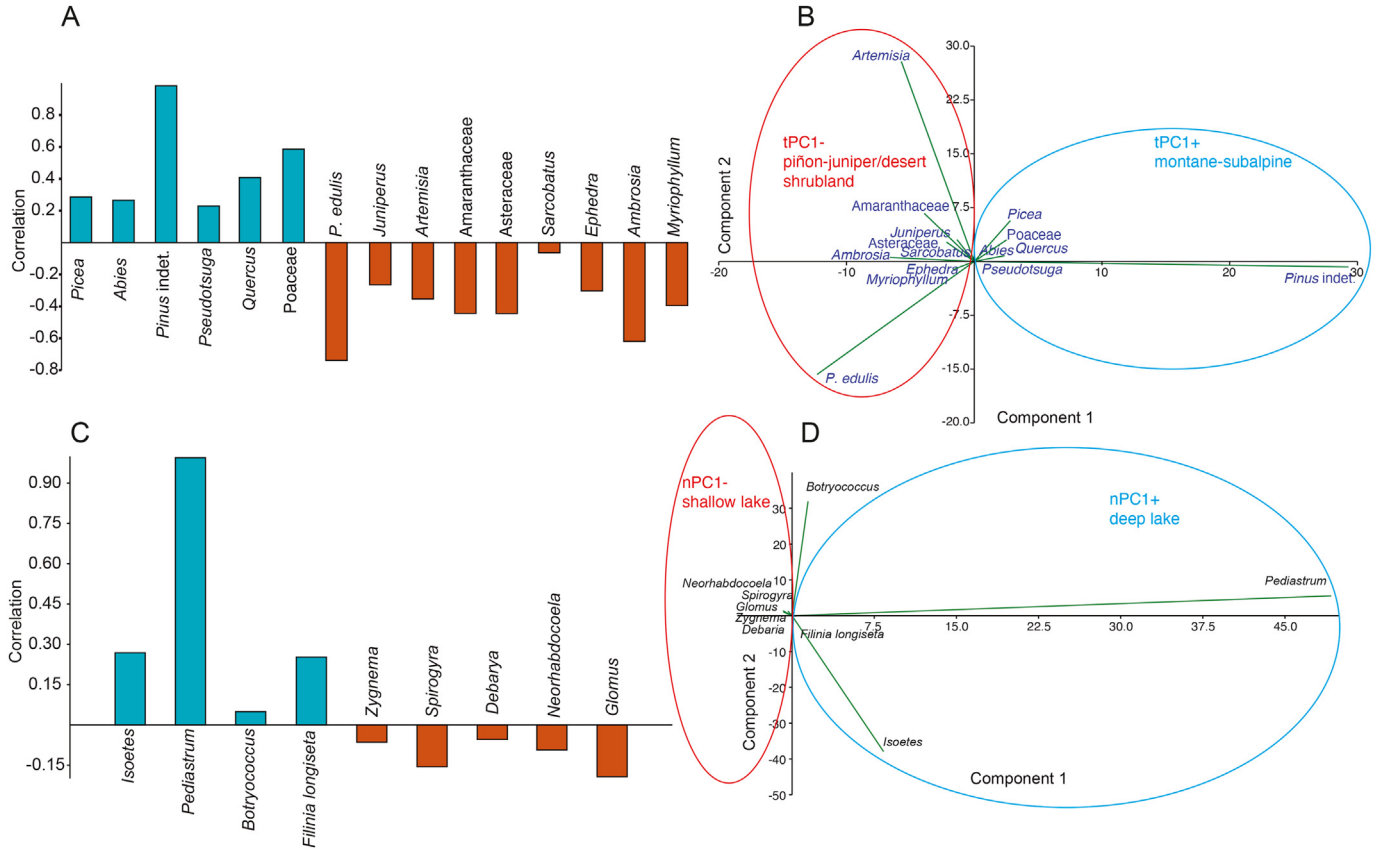

Fig. 5. Principal component analyses (PCA) from the STL14 terrestrial pollen data (tPCA; A and B) and NPP data (nPCA; C and D). A PCA correlation loading (to component 1) and scatter diagrams are shown in A/C and B/D, respectively. The analysis was carried out using PAST 4.10 (Hammer et al., 2001). Interpreted PCA groups are shown (see text for explanation).

4.1. MIS5 (including the LIG, between ~130 and 73 kyr; 900-610 cm depth)

MIS5 is generally characterized by the abundance of taxa in the tPC1- pollen group, dominated by *P. edulis*, *Ambrosia* and *Artemisia* and, in lower abundance, Amaranthaceae and *Juniperus* (Fig. 3). *Picea* and *Quercus* are found in only small quantities, which, for the former, is reflected in the high *Artemisia*/*Picea* (A/P) ratio, reaching a maximum between ~120 and 108 kyr (Fig. 6). The rooted aquatic macrophyte *Myriophyllum* is abundant during this period as well as the NPPs *Spirogyra, Neorhabdocoela* and *Glomus* (Fig. 4).

Several orbital-scale cyclic changes are observed in the pollen during MIS5 shown by decreases in the abundance of the species of the tPC1- group, changes in the A/P ratio and *P. edulis* + *Juniperus* abundances, and small increases of group tPC1+. For example, *Picea* and/or *Pinus* indet. increased between ~126 and 123 kyr, between 101-96 kyr and 90-85 kyr, which are accompanied by enhancements in NPP PC1+ group with taxa such as *Pediastrum*. Charcoal particles and concentration are high during MIS5e and show a decreasing trend over the rest of MIS5 (Fig. 4).

4.2. MIS4 (between 73 and 58 kyr; 610-465 cm)

MIS4 began with an important vegetation change: a significant increase in pollen of the group tPC1+, especially *Pinus* indet., which replaced *P. edulis* and became the most abundant conifer around Stoneman Lake (Figs. 3 and 6). *Pinus* indet. showed the maximum abundance of the entire record at ~60 kyr. At the same time, there was a significant increase in *Picea*, reflected in a lower A/P ratio, an increase in nPC1+ algae of *Pediastrum*, and significant expansion of both *Isoetes* and *Botryoccocus*. *Myriophyllum* decreased considerably during this period, together with *Spirogyra* and *Glomus*. Charcoal particles and concentration showed low occurrences during MIS4.

4.3. MIS3 (between 58 and 27 kyr; 465-302 cm)

This period was characterized by significant changes in the environment with three main palynological oscillations (MIS3c, b and a; Figs. 3, 4 and 6). During MIS3c, an increase in the pollen of plants of group tPC1- occurred. *Artemisia* and Amaranthaceae pollen percentages reached their maximum for the entire record and produced an increase in the A/P ratios. *Pinus* indet. showed a significant decrease then. MIS3b was characterized by an increase in *Pinus* indet. and *Picea* and thus in the tPC1+ group and a minimum in the A/P ratio. During MIS3a, *P.* indet. showed a decrease, and an increase in the pollen of plants of group tPC1-, mostly in *Artemisia* but also in *P. edulis,* occurred. NPP PC1+ group increased during MIS 3 and shows oscillations similar to the terrestrial pollen PC1, with two maxima during 3c and 3a and a minimum during 3b. In general, the occurrences of *Glomus, Zygnema, Spirogyra* and *Neorhabdocoela* are minimal during MIS3. The resting eggs of the rotifer *Filinia longiseta* were abundant during MIS3c, showed maximum abundances during MIS3a, and were largely absent during MIS3b. Charcoal particles were at a maximum during MIS3c and decreased over the rest of MIS3, followed by another peak at the end of MIS3a.

4.4. MIS2 (including the Last Glacial Maximum, between 27 and 15 kyr; 302-272 cm)

MIS2 was characterized by a decrease in *Pinus* indet., an increase in *Picea* and *Abies* and an increase in *Artemisia*, which triggered an overall decrease in taxa of the tPC1- group. Algae, especially *Pediastrum* and thus nPC1+, increased considerably at this time showing the highest values of the record (Figs. 4 and 6). *Isoetes* and *Filinia longiseta* also show peak values. A minimum in charcoal is observed during this period, with values comparable to MIS4.

4.5. MIS1 (including the Bolling-Allerod (B-A), Younger Dryas (YD) and Holocene (15-0 kyr; 272-0 cm)

Picea and *Abies* decreased considerably and *Pinus* indet. shows a decreasing trend during this period (Fig. 3). The decrease in *Picea* triggered an increase in the A/P ratio, which stays high during MIS1 (Fig. 6). *Quercus* reached highest abundances during this period. Taxa of the tPC1- group such as *Ambrosia*, Asteraceae, Amaranthaceae and *Juniperus*, as well as the aquatic plants Cyperaceae and *Myriophyllum*, show increasing trends throughout the Holocene. *Pediastrum* and *Isoetes* decreased considerably and the NPP taxa from group PC1-, including *Zygnema*, *Spirogyra*, *Neorhabdocoela* and *Glomus*, increased reaching maxima in the last 5 kyr. *Botryococcus* exhibits an increasing trend, reaching a peak at ~6.5 kyr, and subsequently decreased during the Late Holocene until present. Charcoal particles increased during MIS1, especially in the Middle and Late Holocene, and reached their maximum values of the record at ~1 kyr, including large charcoal particles (Fig. 4).

5. Discussion

Previous studies show that each vegetation type in Arizona is characterized by its own unique pollen rain so that paralleling the zonation of vegetation there are corresponding changes in the composition of the modern pollen rain (Hevly, 1968). Therefore, the modern pollen rain can be used as an index of modern climate and previous works compared modern and fossil pollen spectra to reconstruct past vegetation and climate in Arizona (Davis and Shafer, 1992; Anderson, 1993). Pollen records from Rocky Mountain alpine and montane wetlands show that vegetation was highly sensitive to climate variability during recent glacial-interglacial cycles due to orbital- and millennial-scale variability (Jiménez-Moreno et al., 2007a, 2008, 2011, 2020, 2021; Anderson et al., 2014; Jiménez-Moreno and Anderson, 2013). Tree forest species responded to changes in climate with vertical displacements upwards when climate warmed, and downwards when climate cooled. The movements of the vegetation assemblages during the Pleistocene and Holocene have been recognized by changing pollen abundances. In previous studies, oscillations in the upper and lower limits of the forest were interpreted as resulting from millennial-scale climatic variations. Several synthetic pollen relationships or ratios can be used as proxies for changes in vegetation and climate oscillations. For example, the A/P (*Artemisia*/*Picea*) ratio points to the relative changes in elevation between the subalpine altitudinal bioclimatic assemblage and lower elevation steppe vegetation mostly driven by changes in temperature (Fig. 1; Carrara et al., 1984; Toney and Anderson, 2006; Jiménez-Moreno et al., 2011, 2020). The increases in *Artemisia*, species of which occur today below the lower montane zone, can be explained as an upward shift of the steppe induced by warming and aridity (Jiménez-Moreno et al., 2011; Jiménez-Moreno and Anderson, 2013). Thermophilous montane taxa such as *P. edulis* and *Juniperus* indicate altitudinal changes of the lower forest-steppe ecotone over time, also controlled primarily by temperature (Cole et al., 2013). Two species of *Pinus* currently grow in the STL area: *P. ponderosa* and *P. edulis*, and both contribute pollen to modern sediments. However, these two species grow across a range of elevations (see Fig. 1) and fluctuations in the relative frequency of their pollen in the Pleistocene sediments indicate displacements in elevation due to shifts in climate (i.e., temperature; Hansen and Cushing, 1973).

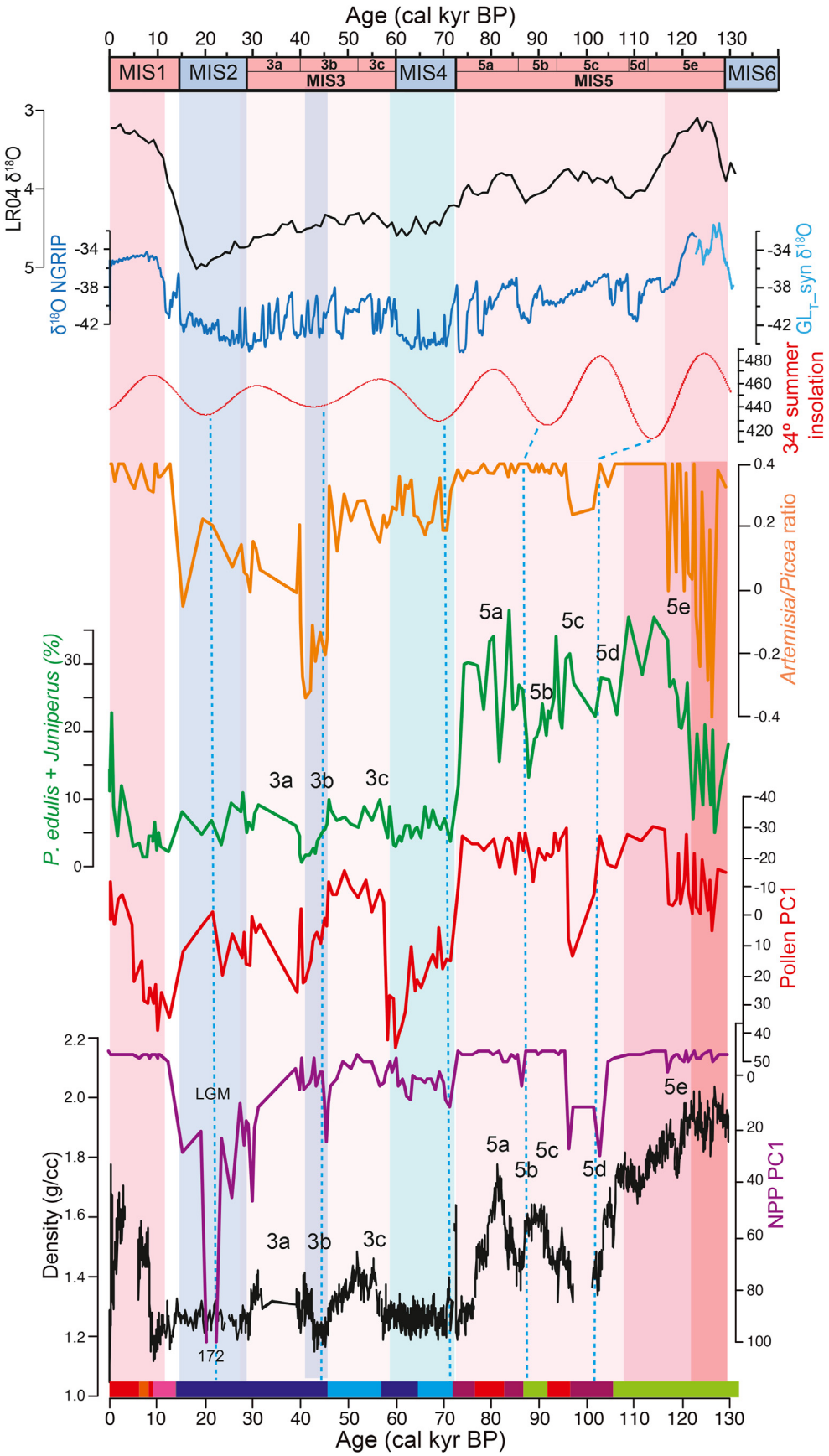

Fig. 6. Comparison of climate and lake level proxies from STL14 (bottom) with summer insolation at 34°N (Laskar et al., 2004), $\delta^{18}O$ values from NGRIP (‰ VSMOW) (NGRIP Members, 2004) and GL_syn $\delta^{18}O$ record (‰ VSMOW) (Barker et al., 2011) and the LR04 $\delta^{18}O$ record (Lisiecki and Raymo, 2005). Ages for Marine Isotope Stages (MIS) at the

Lake levels from SW USA also responded to past climate changes – with higher lake levels during cold and/or humid periods and lower lake levels during warm and/or arid periods – mostly triggered by changes in the precipitation-evaporation balance (Allen and Anderson, 2000; Fawcett et al., 2011; Jiménez-Moreno et al., 2007a; Yuan et al., 2013; Shuman and Marsicek, 2016; Staley et al., 2022). Aquatic macrophytes (*Myriophyllum*, *Isoetes*), algae (*Pediastrum*, *Botryococcus*, *Spirogyra*, *Zygnema*) and other organisms (such as the rotifer *Filinea longiseta* and the aquatic flatworm *Neorhabdocoela*) are conditioned by lake level and shore surface area. The abundances of these aquatics changed through the different climatic stages, providing us with information about lake depth, nutrients and productivity. *Pediastrum*, a colonial alga, has been interpreted as an indicator of oligotrophic to mesotrophic deepwater lake conditions (Nielsen and Sorensen, 1992; Kaufman et al., 2010; Anderson et al., 2020). *Botryoccocus*, also a colonial green microalga, has previously been interpreted as a shallow and eutrophic water indicator (Batten and Grenfell, 1996; Guy-Ohlson, 1992; Jiménez-Moreno et al., 2007b). High abundances of *Glomus* endomycorrhizal fungus in sediment samples from paleoecological records have been related to increased rates of soil erosion and other mechanical soil disturbances (Anderson et al., 1984; Van Geel et al., 1989).

This study shows that vegetation and aquatic organisms living in the STL environment responded very sensitively to climate changes that occurred in the last ~130 kyr. However, because we have tuned the STL14 record to the LR04 global mean benthic isotope stack (Lisiecki and Raymo, 2005) in the older portions of the core beyond radiocarbon dating, the chronologies for the MIS3, 4 and 5 transitions are not independent. This precludes us from studying leads or lags in the paleoenvironmental and paleoclimatic data from STL with respect to other regional or global paleoclimatic records.

5.1. Last interglacial (LIG) - MIS5

The LIG was generally warmer than the Holocene. This can be deduced by the predominance of *P. edulis* and associated plants such as *Juniperus*, *Ambrosia*, Amaranthaceae, Asteraceae and *Artemisia,* which today grow at a lower altitude than the lake (pinyon-juniper and desert shrubland Figs. 2 and 5). This would imply an upwards displacement of the *P. edulis* and *Juniperus* ecotone towards higher altitudes than present. The maximum temperatures of MIS5 would have been reached between 117 and 108 kyr (MIS5e), as shown by the maximum A/P ratio, high *P. edulis* + *Juniperus* and Amaranthaceae. Our results agree with other paleoclimatic records from the western USA that show warmer than present conditions during MIS5e, such as the palynological records from Bear Lake in Utah (Jiménez-Moreno et al., 2007a), Carp Lake in Washington (Whitlock and Bartlein, 1997), Ziegler Reservoir in Colorado (Anderson et al., 2014), and Clear Lake in California (Adam et al., 1981) (Fig. 6). MIS5e is also globally recognized as a warmer interglacial than the Holocene (Past Interglacials Working Group of PAGES, 2016).

We can distinguish 5 climatically distinct periods during MIS5, with three warmer substages corresponding to MIS5e, 5c and 5a and two intervening cooler substages corresponding to MIS5d and 5b. These climatic oscillations were most likely forced by precession-related changes in insolation (Laskar et al., 2004) and therefore show similar trends to the Marine Isotope Stages (Lisiecki and Raymo, 2005) and the isotopic data from Greenland: $\delta^{18}O$ values from NGRIP (NGRIP Members, 2004) and GL_syn $\delta^{18}O$ record (Barker et al., 2011) (Fig. 6). Even though the vegetation changes inferred from the pollen in the STL14 record appear to correlate well with the main global climatic patterns during MIS5, there are differences in the timing of the main climatic phases with respect to the insolation and other paleoclimatic records. The STL14 record seems to show a delay in the response of the vegetation with respect to the timing of temperature maximum and insolation maxima and minima during MIS5e-5b (Fig. 6). This is probably due to the uncertainty in the chronology for this part of the record, which is based only on tuning of facies changes with LR04 tie-points at MIS5/4 and MIS6/5 transitions (Table 1; Fig. 2).

The driest conditions, shown by the abundance of shallow lake NPP indicators nPC1-, occurred coincident with the warmest phase of the LIG during MIS5e, related to summer insolation maxima (Fig. 6). However, pollen data from the period between 130 and 117 kyr indicate a vegetation characteristic of higher elevations consistent with somewhat "colder" conditions than later on between 117 and 108 kyr (Fig. 6). This is deduced by the lower A/P ratio, higher *Pinus* indet., and thus pollen tPC1+, and lower *P. edulis* + *Juniperus* abundance with respect to the earlier period. The shallow lake massive clay-silt sedimentary facies and peak density values show that the MIS5e would have started at 130 kyr and highest density values are reached between 130 and 117 kyr, disagreeing with the pollen. This asynchronicity between the sedimentation and palynological record for the earliest part of MIS5e could have been due to especially warm and dry conditions in the STL area during summer insolation maxima (Fig. 6). Such conditions could have produced enhanced aridity and drought, low lake levels indicated by low algae values, opening of the vegetation in the surroundings of the lake triggering an increase in erosion deduced by peaks in *Glomus* between 123 and 118 kyr and could have produced a bias in the pollen sedimentation and resedimentation of older pollen into the lake pointing to "colder" climatic conditions. This agrees with the abundant inorganic content in the studied samples and visually observed pollen concentration and preservation at that time, which is quite poor. A previous study of mid-Pleistocene lacustrine sediment from the Valles Caldera, New Mexico, found that the driest conditions and megadroughts occurred during the warmest phases of past interglacials (Fawcett et al., 2011), which would agree with our interpretation.

STL lake levels were generally low during the entire MIS5 period. This can be interpreted by the types of aquatic algae present then, mostly dominated by *Botryococcus* and *Spirogyra*, and low nPC1+. *Myriophyllum* was abundant, indicating sediments deposited in shallow waters, as it is currently most often found in water of 0.5–2.5 m of depth with abundant nutrients (Gross et al., 2020) and can withstand considerable desiccation (Cook, 2004). Stages MIS5d and MIS5b can be interpreted as colder periods, with lower evaporation rates and resulting increases in lake levels, as reflected in enhanced abundances of planktonic algae such as *Pediastrum* and *Botryococcus* and thus nPC1+. Both greater erosion (increases in *Glomus*) and nutrient supply to the lake with increased eutrophication (*Spirogyra* and *Zygnema*) are observed during the warm stages MIS 5e, 5c and 5a and showing an increasing trend towards more recent stages. The increases in *Spirogyra* and *Zygnema* indicate the development of important masses of filamentous algae in the lake, suggesting eutrophic stagnant shallow water under milder climate and longer snow free periods (Carrión, 2002).

very top of the figure come from Camuera et al. (2019). Correlations between the STL14 record with MIS stages are attempted through shadings and dashed lines. The different shades of pink point to relative warmth (the darker the warmer). The same applies for blue shading, representing cooler temperatures. Numbers with letters show the identification of MIS substages in the STL14 record.

Neorhabdocoela was abundant during the warmest and driest stages of MIS5, also pointing to shallow and eutrophic lake conditions. This is inferred because *Neorhabdocoela* is restricted to the phytal zone (feeding for example on Rotatoria and diatoms) and produces oocytes - thick-walled resting-eggs - for propagation and for surviving unfavorable ecological conditions during drought (Haas, 1996).

Fire activity also changed with insolation and climate during MIS5 (Fig. 6). It was especially high during MIS5e and local fires most likely occurred in the STL area, deduced by the occurrence of large charcoal particles. Fire activity diminished during MIS5d, and showed a decreasing trend over the rest of MIS5 with slight increases during MIS5c and MIS5a. This pattern of increasing charcoal deposition during MIS5e and the warm interstadials MIS5a and 5c agrees with other charcoal records from SW North America such as the Snowmastodon (Ziegler reservoir; Anderson et al., 2020) and the Baldwin Lake (Glover et al., 2020) records. However, fire activity during the last interglacial was lower than during MIS3 and the Holocene in the STL record (Fig. 4). This pattern is also observed in the charcoal record from Baldwin Lake (Glover et al., 2020). A positive relationship between montane and subalpine *Pinus* abundance and charcoal production was previously observed in Colorado (Jiménez-Moreno et al., 2019; Anderson et al., 2020). Perhaps the charcoal abundance was lesser during MIS 5, dominated by the lower elevation *P. edulis* vegetation, than during stages MIS3 and MIS1, characterized by the abundance of ponderosa pine, because these later pines are more fire-prone and fire-adapted species (Fitzgerald, 2005) (Fig. 3).

5.2. MIS 4. onset of the last glaciation

Rapid and significant cooling occurred at the MIS5/4 boundary in the STL record. This is deduced by the substantial increase in *Pinus* indet. pollen (possibly *P. ponderosa*, the higher elevation *Pinus* species growing in the STL area at present but also *P. flexilis* or *P. strobiformis*), which probably expanded in the STL area and replaced *P. edulis* (piñon) (Figs. 3 and 6). This indicates a considerable vertical displacement of forest species including the montane ecotype of *P. ponderosa* (currently at elevations between 2000 and 2400 m) towards lower altitudes and around the lake. Climatic cooling is also supported by the increase in *Picea* in the pollen spectra, indicating a regional expansion or closer proximity of upper montane forest to STL. The STL14 pollen record shows a distinct rapid cooling pattern during MIS4, different than the typical saw-tooth structure of the glacial cycles with long and gradual glaciations that is observed in other paleoclimatic pollen records from western North America (Fig. 7). Perhaps the steep gradient in elevation in the STL area and the proximity of small populations in microsites favored fast and significant vegetation changes in the area with climate change.

Lake level increased synchronously with the vegetation change due to the cooling and reduced evaporation, producing an increase in algal remains of *Botryoccocus, Isoetes* and *Pediastrum* and thus nPC1+ (Figs. 4 and 6). Lower erosion rates and reduced nutrient supply into the lake can be deduced from the decrease in *Glomus* and *Spirogyra*, respectively. A deepening of the lake also agrees with the increase in abundance of *Isoetes*, probably related to an expansion of the shallow water lakeshore area.

Fire activity was considerably diminished in the area with the cooling and increase in effective precipitation. This agrees with other regional fire proxy records that indicate little, if any, fire occurrence during MIS 4 (Anderson et al., 2020; Glover et al., 2020). Lower summer insolation controlled by orbital-scale precession changes at this latitude (34°N; Fig. 6) most likely contributed to the lower regional fire occurrence.

5.3. MIS 3. a relatively warm period during the last glaciation

MIS3 is characterized by a climatic warming that interrupted the trend towards colder conditions registered in the previous MIS4 period. This is deduced by the increase in thermophilous plants of the tPC1pollen group - such as *Artemisia* (the A/P index) and Amaranthaceae. The pollen record indicates cyclical climatic oscillations, and we can subdivide MIS3 into three substages, two warm (MIS3c and a) and one cold (MIS3b), based on warmer environment (lower-elevation steppe) versus colder environment (higher-elevation montane *Pinus* indet. and subalpine *Picea*) pollen taxa, and variation in sedimentation (MS and density; Figs. 1 and 2) and aquatic algae (Figs. 3, 4 and 6).

Percentages of *Picea* of 15–20% during MIS3b are similar to present values of this taxon in subalpine forests of the Rocky Mountains (Anderson et al., 2014; Jiménez-Moreno et al., 2019). This shows that this subalpine forest species must have existed in the STL area or nearby, implying a significant movement of the vegetation towards lower elevation due to climatic cooling. Temperatures increased again during MIS3a, deduced by the increase in the plants of group tPC1-, pointing to an upwards displacement of the vegetation.

Lake levels increased over the course of MIS3b, indicated by the increase in deep-lake algae such as *Pediastrum* (and NPP nPC1+). Superimposed on this trend are significant fluctuations mirroring the terrestrial vegetation oscillations, indicating that water depth was mostly controlled by temperature fluctuations and related oscillations in effective precipitation. The increases in *Isoetes* during stages 3c and the end of 3b and 3a, exhibit oscillations similar to the climate, and indicate that the lake waters were very clear and oligotrophic, environments preferred by this plant, during those times. Minimum values of *Glomus* and *Spirogyra* support this interpretation and indicate minor contributions of allochthonous material from erosive events and a limited supply of nutrients into the lake. The eggs of the rotifer *Filinia longiseta* increased in MIS3c and MIS3a, supporting indications of increasing lake levels, since this planktonic species inhabits pelagic environments in open and sparsely vegetated lakes (Van Geel, 2001).

Fire activity increased during MIS3c, with a peak around 55 kyr, and decreased during the rest of MIS3 (Fig. 4). This could have been due to warmer and drier conditions indicated by the pollen during that substage. Charcoal records for MIS3 in SW North America are rare, but significant fire activity has also been recorded between 56 and 50 kyr in Baldwin Lake (California; Glover et al., 2020) and between 57 and 47 kyr in Lake Chalco (Mexico), both related to a summer insolation maximum at that time (Martínez-Abarca et al., 2021) and pointing to a regional North American pattern in fire activity.

5.4. MIS 2. Last Glacial Maximum (LGM)

Colder conditions were reached during MIS2, shown by the high abundance of *Picea* and *Abies* between 25 and 30%, which indicates that they probably occurred in the vicinity of STL at that time (Anderson, 1993; Anderson et al., 2014). This implies a total vertical displacement of ~1000 m of the subalpine vegetation towards lower altitudes due to the decrease in temperatures between MIS5 and MIS2. Accompanying this climate cooling was a significant rise in the lake level, most likely due to the low evapotranspiration and an increase in Pacific moisture during boreal winter in the SW USA due to the intensification and displacement of the polar jet stream to the south of its present position (COHMAP Members, 1988; Schmidt and Hertzberg, 2011; Oster et al., 2016; Amaya et al., 2022). This is indicated by the considerable increase in deep-lake algae such as *Pediastrum*, and the rotifer *F. longiseta*, which reached

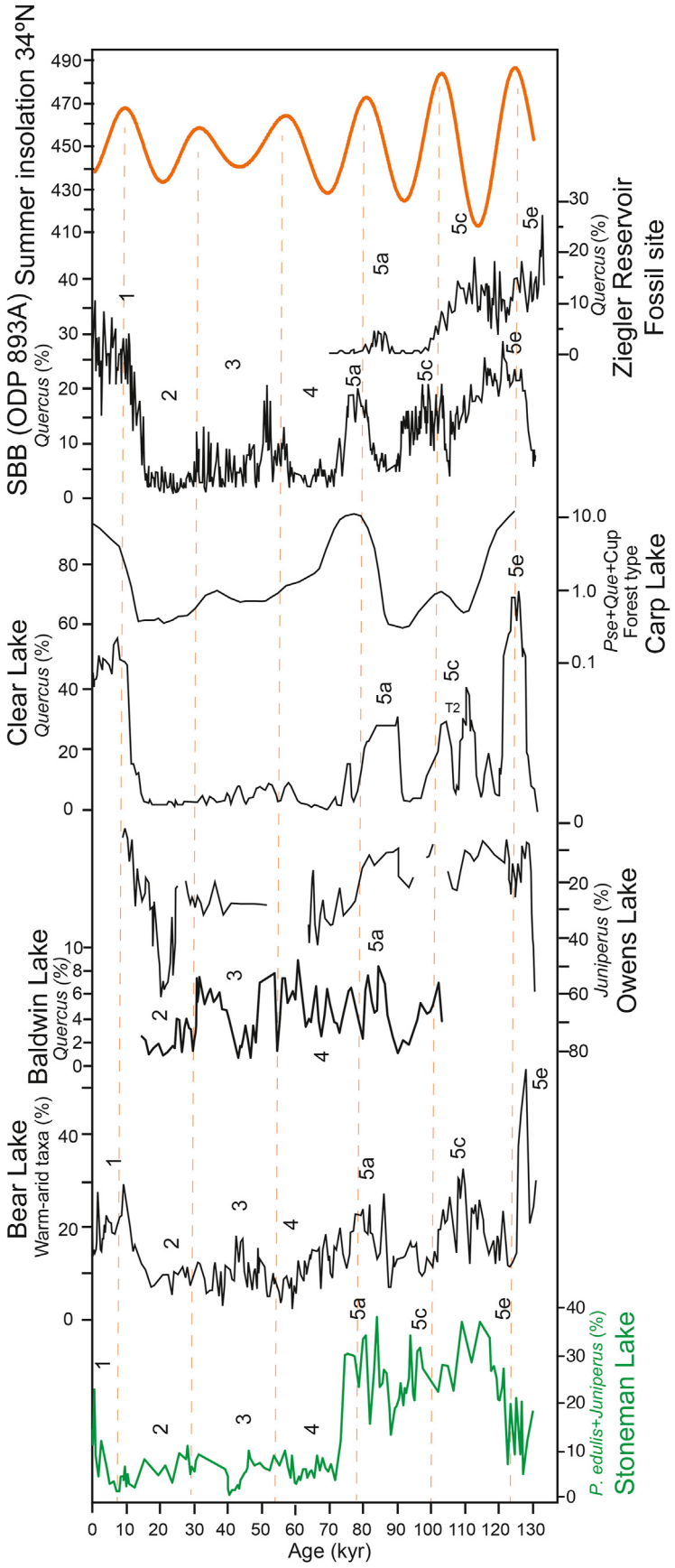

Fig. 7. Comparison of long pollen records from Western USA for the last 130 kyr with summer insolation for 34°N (Laskar et al., 2004). Pollen data are from Bear Lake, Utah–Idaho (Jiménez-Moreno et al., 2007a); Owens Lake, California (Woolfenden, 2003); Clear Lake, California (Adam et al., 1981); Carp Lake, Washington (Whitlock and Bartlein, 1997); and

maximum abundances here. The greatest abundance of *Pediastrum* and nPC1+ shows that during the LGM, lake levels were probably the highest of the last 130 kyr. A deepening of the lake also agrees with the increase in abundance of *Isoetes*, a clear- and oligotrophic-water fern indicator (Kaufman et al., 2010), consistent with an expansion of the lakeshore area.

Fire activity was very low at this time (Fig. 4). This agrees with other regional and global charcoal records showing that fire was consistently lower during the LGM than during previous MIS5 and MIS3 stages (Power et al., 2008; Daniau et al., 2010; Glover et al., 2020) and supports the strong relationship between insolation, global temperature and fire activity. Colder and more humid conditions would have reduced the potential for fire ignition and spread, probably reducing the frequency of fires and thus charcoal production.

5.5. MIS 1. deglaciation (including the B-A and YD) and Holocene

A significant climate warming occurred during MIS1, which forced a shift of forest species towards higher altitudes resulting in the displacement of the subalpine forest around STL with montane forest species. This is deduced by the decrease in *Picea* (increase in A/P ratio) and the significant increase in *Pinus* indet. (most-likely *P. ponderosa* in this case) and *Quercus*, which colonized the STL area (Figs. 3 and 6). We are unsure if the observed warming represents the glacial termination or the Holocene. This is due to the sampling resolution, which is not high enough to recognize the distinct climatic intervals of the deglaciation such as the B-A and YD. A thermal peak was reached during the Holocene, however, temperatures were never as high as during the LIG (MIS5e). This interpretation comes from the fact that *P. edulis* never reached the abundance of the LIG and the piñon-juniper vegetation remained at lower elevations during the Holocene until present. Our finding at STL agrees with other long pollen records from W US such as Bear Lake in Utah (Jiménez-Moreno et al., 2007a), Carp Lake in Washington (Whitlock and Bartlein, 1997) Ziegler Reservoir in Colorado (Anderson et al., 2014) and Clear Lake in California (Adam et al., 1981) (Fig. 6).

The climate stayed quite warm (A/P ratios) throughout the Holocene, although some millennial climatic variations are observed. The lake level lowered considerably, interpreted by the abrupt decrease in the abundance of aquatic algae (*Pediastrum*), plants (*Isoetes*) and rotifers (*F. longiseta*) from nPC1+. This was probably due to the increase in temperatures and greater evaporation and the displacement of the jet stream to the north, producing a decrease in Pacific winter precipitation (Harrison et al., 2003). Vegetation and NPP patterns show that climate (temperature or precipitation) changed. A warmer but still cool and relatively humid Early Holocene is deduced by the high abundance of *Pinus* indet. and the abundance of *Botryococcus*, indicating the presence of a shallow lake. A tendency toward warmer conditions, aridification and decrease in lake levels is observed since ~6 kyr, interpreted by the increase in thermophilic-xerophilous species of the PC1- group and the decrease in the *P. ponderosa* forests and *Botryococcus* since the Middle Holocene, as Hasbargen (1994) previously observed. A greater contribution of allochthonous detrital and nutrient materials is observed from this moment on, interpreted from the increase in *Glomus* and *Spirogyra* and *Zygnema*. Finally, the increase in the aquatic plant *Myriophyllum* supports the interpretation of a shallow and very eutrophic lake in the Late Holocene.

Another distinct feature of the Holocene pollen record with respect to the LIG is the abundance of *Quercus* in the current interglacial. *Quercus* has previously been interpreted as a thermophilous indicator in montane and alpine sedimentary records, increasing during interglacials and interstadials (Jiménez-Moreno et al., 2007a, 2010; Fawcett et al., 2011; Glover et al., 2020). *Quercus* presently occurs within the *P. ponderosa* forest vegetation belt and seems to have been favored in this area by warm Holocene climate and environmental conditions. The increase in *Quercus* during the Holocene was perhaps also favored by enhanced fire activity in the Holocene (see below) as has been observed in other pollen records from the SW US (Fall, 1985, 1988, 1997a,b; Jiménez-Moreno et al., 2011; Johnson et al., 2013). An increase in the abundances of *P. edulis* and *Juniperus* forest species is also observed over the last ~6 kyr (Fig. 3). Previous studies show that the expansion of *P. edulis* since 6 kyr is a widespread phenomenon in the SW USA (see synthesis in Jiménez-Moreno et al., 2021) and was related to changes in insolation and enhanced El Niño-winter precipitation in this region.

Certain of these vegetation trends are likely to continue, as many plant species are shifting towards higher elevations due to recent global warming in mountain regions (IPCC, 2022). The forecasted climate warming scenarios for the next decades (IPCC, 2022) will most-likely trigger further expansion of *P. edulis* and *Juniperus* (only 100–200 m below STL) and other forest species towards higher elevation areas than at present, occupying the study area in a similar way as during the LIG.

Fire activity was low at the beginning of the Holocene, but showed an increasing trend in the Middle to Late Holocene, with maxima of fire activity including local fires (shown by the occurrence of large charcoal particles) at ~6.5 and 1 kyr (Fig. 4). Charcoal deposition increased but was delayed with respect to maxima in summer insolation and pine forest at ~10 kyr by ~3500 years (Figs. 3, 4 and 6). This could suggest that Holocene fire activity initiated after the initial stages of forest development there, as climate warmed and fuel accumulated. This first peak in fire activity coincides with the timing of the warmest period of the Holocene in this region (Shuman and Marsicek, 2016), and agrees with other charcoal records from Colorado such as Hermit Lake (charcoal maxima at ca. 6.6–4.4 ka; Anderson et al., 2018) or De Herrera Lake (Anderson et al., 2008). A second peak in fire activity coincides in time with the Medieval Climate Anomaly (MCA). This period has previously been identified as especially active in fire activity in the Rockies due to especially warm and droughty conditions (Calder et al., 2015; Jiménez-Moreno et al., 2021) but could have also been due to activity in the area by Southwest Native Americans (Pilles, 1996; Cordell and McBrinn, 2012).

6. Conclusions

The detailed palynological analysis of the STL14 sedimentary record in Arizona permitted us to learn about vegetation, environment, and climate changes since the LIG in the SW USA. Although the chronological control of our record is incompletely independent beyond MIS3, the pollen data show that vegetation changed largely conditioned by orbital-scale changes in insolation, primarily precession. This confirms the link between global climate variations and regional vegetation changes through movements of forest vegetation species upslope or downslope depending on whether climate warmed or cooled, respectively.

The warmest conditions of the last 130 kyr were reached during

ODP 893A, Santa Barbara Basin, California (Heusser, 1998, 2000). Note that each of the time series is plotted against its own age model. The line plotted for Carp Lake is a locally weighted mean and not % abundance as in the other records. The orange dashed lines highlight the time of maxima in summer insolation related to precession cycles.

the LIG, deduced by the abundance of pollen of the *P. edulis* and *Juniperus* vegetation belt, which today grow mostly lower than the lake elevation, indicating their occurrence in the STL area at that time. Climate cooled since then and into the last glaciation closely following orbital-scale precession-forced climate variations. The coldest conditions were reached during MIS2, indicated by the occurrence around the lake of subalpine species such as *Picea* or *Abies*. This confirms (Anderson et al., 2000) a downslope vegetation displacement of about 1000 m with respect to their occurrence at present. Climate warmed up during the last deglaciation and Holocene but never reached the peak temperatures of the LIG.

STL water level oscillations closely match vegetation and climate variations. Lake levels were conditioned by evapotranspiration and the amount of effective Pacific winter precipitation. Low water level occurred during warm interglacial/interstadial phases (i.e., MIS5e, c, a; MIS3c, MIS3a and MIS1) and high lake levels occurred during cold and humid glacial/stadial periods (i.e., MIS5d, MIS4, MIS3b, MIS2). The highest STL water level was recorded during MIS2, coinciding with the LGM.

Although the LIG and Holocene are not exact analogs for future warm climates, due to different orbital configurations, we expect to see a similar vegetation response in the study area to future temperatures in the context of future anthropogenic greenhouse projections, with the *P. edulis* and *Juniperus* vegetation belt moving towards higher elevations than at present and occupying the STL area.

Author contributions

G. Jiménez-Moreno performed the pollen analysis, pollen data interpretation and wrote the paper. R.S. Anderson and P.J. Fawcett retrieved the sedimentary record and worked on the chronological control of the core. S. Staley performed the sedimentary and facies description and interpreted the sedimentary data. All authors contributed to the interpretation, discussed the results and provided inputs to the paper.

Declaration of competing interest

The authors declare that they have no known competing financial interests or personal relationships that could have appeared to influence the work reported in this paper.

Data availability

Data will be made available on request.

Acknowledgements

GJM acknowledges funding from the Ministerio de Ciencia Innovación y Universidades, grant number PRX18/00080 and PRX21/00127, for "Salvador de Madariaga" research stays at the University of New Mexico and Northern Arizona University for the sampling, treatment of sedimentary samples for pollen extraction and pollen analysis of the STL14 core. He also acknowledges funding from projects CGL2013-47038-R and CGL2017- 85415-R of the "Ministerio de Economía y Competitividad of Spain and Fondo Europeo de Desarrollo Regional FEDER", Junta de Andalucía P-20-00059, FEDER Projects B-RNM-144-UGR18 and UGR-FEDER B-RNM-144-UGR18 and the research group RNM-190 (Junta de Andalucía). RSA acknowledges a grant from the Arizona TRIF research program (Project 1002654; "Mega-droughts, climate change and the Southwest: Stoneman Lake, AZ, Paleoenvironments Drilling Project"), as well as assistance from the US Forest Service, for core collection. The authors thank the personnel at UMNs NSF CSD facility for their support. This paper greatly benefited from the reviews of two anonymous reviewers and the editorial work of Donatella Magri.

References

Adam, D.P., Sims, J.D., Throckmorton, C.K., 1981. 130,000-yr continuous pollen record from Clear Lake, lake county, California. Geology 9, 373–377.
Allen, B.D., Anderson, R.Y., 2000. A continuous, high-resolution record of late Pleistocene climate variability from the Estancia basin, New Mexico. Geol. Soc. Am. Bull. 112, 1444–1458.
Alizadeh, M.R., Abatzoglou, J.T., Luce, C.H., Adamowski, J.F., Farid, A., Sadegh, M., 2021. Warming enabled upslope advance in wetsren US forest fires. Proc. Natl. Acad. Sci. USA 118, e2009717118.
Amaya, D.J., Seltzer, A.M., Karnauskas, K.B., Lora, J.M., Xhang, X., DiNezio, P.N., 2022. Air-sea coupling shapes North American hydroclimate response to ice sheets during the Last Glacial Maximum. Earth Planet Sci. Lett. 578, 117271.
Anderson, R.S., 1993. A 35,000 year vegetation and climate history from potato lake, Mogollon Rim, Arizona. Quat. Res. 40, 351–359.
Anderson, R.S., Homola, R.L., Davis, R.B., Jacobson Jr., G.L., 1984. Fossil remains of the mycorrhizal fungal *Glomus fasciculatum* complex in postglacial lake sediments from Maine. Can. J. Bot. 62, 2325–2328.
Anderson, R.S., Betancourt, J.L., Mead, J.I., Hevly, R.H., Adam, D.P., 2000. Middle- and late-Wisconsin paleobotanic and paleoclimatic records from the southern Colorado Plateau. Palaeogeogr. Palaeoclimatol. Palaeoecol. 155, 31–57. USA.
Anderson, R.S., Allen, C.D., Toney, J.L., Jass, R.B., Bair, A.N., 2008. Holocene vegetation & forest fire regimes in subalpine & mixed conifer forests, southern Rocky Mountains, USA. Int. J. Wildland Fire 17, 96–114.
Anderson, R.S., Jiménez-Moreno, G., Ager, T., Porinchu, D., 2014. High-elevation paleoenvironmental change during MIS 4 e 6 in the central Rockies of Colorado as determined from pollen analysis. Quat. Res. 82, 542–552.
Anderson, R.S., Soltow, H.R., Jiménez-Moreno, G., 2018. Postglacial environmental change of a high elevation forest near Hermit Lake, Sangre de Cristo Range of south central Colorado. In: Starratt, S.W., Rosen, M.R. (Eds.), Chapter 13, "From Saline to Freshwater: the Diversity of Western Lakes in Space and Time", vol. 536. Geological Society of America Special Paper, pp. 221–239.
Anderson, R.S., Jiménez-Moreno, G., Belanger, M., Briles, C., 2020. Fire history of the unique high-elevation Snowmastodon (Ziegler Reservoir) site during MIS 6-4, with comparisons of TII to TI in the southern Colorado Rockies. Quat. Sci. Rev. 232, 106213.
Barker, S., Knorr, G., Edwards, L., Parrenin, F., Putnam, A.E., Skinner, L.C., Wolff, E., Ziegler, M., 2011. 800,000 years of abrupt climate variability. Science 334, 347–351.
Batten, D.J., Grenfell, H.R., 1996. Botryococcus. In: Jansonius, J., McGregor, D.C. (Eds.), Palynology: Principles and Applications, vol. 1. American Association of Stratigraphic Palynologists Foundation, pp. 205–214.
Beug, H.J., 1961. Leitfaden der Pollenbestimmung, vol. 1. Fischer, Stuttgart, p. 63.
Brown, D.E., Lowe, C.H., 1978. Biotic Communities of the Southwest. U.S. Department of Agriculture Forest Service General Technical Report RM-41, scale 1: 1,000,000.
Brown, D.E., Lowe, C.H., 1982. Biotic communities in the American southwest-United States and Mexico. Desert plants 4 (1–4), 1–34.
Brovkin, V., Bruecher, T., Kleinen, T., Zaehle, S., Joos, F., Roth, R., Spahni, R., Schmitt, J., Fischer, H., Leuenberger, M., Stone, E.J., Ridgwell, A., Chappellaz, J., Kehrwald, N., Barbante, C., Blunier, T., Jensen, D.D., 2016. Comparative carbon cycle dynamics of the present and last interglacial. Quat. Sci. Rev. 137, 15–32.
Calder, J., Stopka, C., Parker, D., Jiménez-Moreno, G., Shuman, B.N., 2015. Medieval warming initiated exceptionally large wildfire outbreaks in the Rocky Mountains. Proc. Natl. Acad. Sci. USA 112, 13261–13266.
Camuera, J., Jiménez-Moreno, G., Ramos-Román, M.J., et al., 2019. Vegetation and climate changes during the last two glacial-interglacial cycles in the western Mediterranean: a new long pollen record from Padul (southern Iberian Peninsula). Quat. Sci. Rev. 205, 86–105.
Capron, E., Govin, A., feng, R., Otto-Bliesner, B.L., Wolff, E.W., 2017. Critical evaluation of climate syntheses to benchmark CMIP6/PMIP4 127 ka Last Interglacial simulations in the high-latitude regions. Quat. Sci. Rev. 168, 137–150.
Carrión, J.S., 2002. Patterns and processes of Late Quaternary environmental change in a montane region of southwestern Europe. Quat. Sci. Rev. 21, 2047–2066.
Carrara, P.E., Mode, W.N., Rubin, M., 1984. Deglaciation and postglacial timberline in the san juan mountains, Colorado. Quat. Res. 21, 42–55.
Cayan, D.R., Redmond, K.T., Riddle, L.G., 1999. ENSO and hydrology extremes in the western United States. J. Clim. 12, 2881–2893.
Cayan, D.R., Das, T., Pierce, D.W., Barnett, T.P., Tyree, M., Gershunov, A., 2010. Future dryness in the southwest US and the hydrology of the early 21st century drought. Proc. Natl. Acad. Sci. USA 107, 21271–21276.
COHMAP Members, 1988. Climatic changes of the last 18,000 Years: observations and model simulations. Science 241, 1043–1052.
Cole, K.L., Fisher, J.F., Ironside, K., Mead, J.I., Koehler, P., 2013. The biogeographic histories of *Pinus edulis* and *Pinus monophylla* over the last 50,000 years. Quat. Int. 310, 96–110.

Cook, C.D.K., 2004. Aquatic and Wetland Plants of Southern Africa. Backhuys Publishers, Leiden, The Netherlands.
Cordell, L.S., McBrinn, M.E., 2012. Archaeology of the Southwest, third ed. Routledge.
Cronin, Thomas M., 2010. Paleoclimates: Understanding Climate Change Past and Present. Columbia University Press, 2010.
Dohm, J.M., 1995. Origin of Stoneman Lake, and Volcano-Tectonic Relations of Mormon and San Francisco Volcanic Fields, Arizona. M.S. Thesis. Northern Arizona University, p. 101. Flagstaff, Arizona.
Daniau, A.L., Harrison, S.P., Bartlein, P.J., 2010. Fire regimes during the last glacial. Quat. Sci. Rev. 29 (21–22), 2918–2930.
Davis, O.K., Shafer, D.S., 1992. A Holocene climatic record for the sonoran desert from pollen analysis of montezuma well, Arizona, USA. Palaeogeogr. Palaeoclimatol. Palaeoecol. 92, 107–119.
Diffenbaugh, N., Giorgi, F., 2012. Climate change hotspots in the CMIP5 global climate model ensemble. Clim. Change 114, 813–822.
Djamali, M., Cilleros, K., 2020. Statistically significant minimum pollen count in Quaternary pollen analysis; the case of pollen-rich lake sediments. Rev. Palaeobot. Palynol. 275, 104156.
Faegri, K., Iversen, J., 1989. Textbook of Pollen Analysis. Wiley, New York.
Fall, P.L., 1985. Holocene dynamics of the subalpine forest in central Colorado. AASP Contrib. Ser. 16, 31–46.
Fall, P.L., 1988. Vegetation Dynamics in the Southern Rocky Mountains: Late Pleistocene and Holocene Timberline Fluctuations. PhD Diss. Univ. Arizona, Tucson.
Fall, P.L., 1997a. Fire history and composition of the subalpine forest of western Colorado during the Holocene. J. Biogeogr. 24, 309–325.
Fall, P.L., 1997b. Timberline fluctuations and late Quaternary paleoclimates in the southern Rocky Mountains, Colorado. Geol. Soc. Am. Bull. 109, 1306–1320.
Fawcett, P.J., Werne, J.P., Anderson, R.S., Heikoop, J.M., Brown, E.T., Berke, M.A., Smith, S., Goff, F., Hurley, L., Cisneros-Dozal, L.M., Schouten, S., Sinninghe Damsté, J.S., Huang, Y., Toney, J., Fessenden, J., WoldeGabriel, G., Atudorei, V., Geissman, J.W., Allen, C.D., 2011. Extended megadroughts in the southwestern United States during Pleistocene interglacials. Nature 470, 518–521.
Fitzgerald, S.A., 2005. Fire Ecology of Ponderosa Pine and the Rebuilding of Fire-Resilient Ponderosa Pine Ecosystems. USDA Forest Service Gen. Tech. Rep. PSW-. GTR-198.
Glover, K.C., Chaney, A., Kirby, M.E., Patterson, W.P., MacDonald, G.M., 2020. Southern California vegetation, wildfire and erosion had nonlinear responses to climatic forcing during the Marine Isotope Stages 5-2 (120-15 ka). Paleoceanogr. Paleoclimatol. 35, e2019PA003628.
Gross, E.M., Groffier, H., Pestelard, C., Hussner, A., 2020. Ecology and environmental impact of *Myriophyllum heterophyllum*, an aggressive invader in European waterways. Diversity 12, 127.
Grimm, E.C., 1987. CONISS: a FORTRAN 77 program for stratigraphically constrained cluster analysis by the method of incremental sum of squares. Comput. Geosci. 13, 13–35.
Guy-Ohlson, D., 1992. *Botryococcus* as an aid of the interpretation of palaeoenvironment and depositional processes. Palaeogeogr. Palaeoclimatol. Palaeoecol. 71, 1–15.
Hammer, O., Harper, D.A.T., Ryan, P., 2001. Past: paleontological statistics software package for education and data analysis. Palaeontol. Electron. 4 (1), 9.
Hansen, B.S., Cushing, E.J., 1973. Identification of pine pollen of late quaternary age from the chuska mountains, New Mexico. Geol. Soc. Am. Bull. 84, 1181–1200.
Harrison, S.P., Kutzbach, J.E., Liu, Z., Bartlein, P.J., Otto-Bliesner, B., Muhs, D., Prentice, I.C., Thompson, R.S., 2003. Mid-Holocene climates of the Americas: a dynamical response to changed seasonality. Clim. Dynam. 20, 663–688.
Hasbargen, J., 1994. A Holocene paleoclimatic and environmental record from Stoneman lake, Arizona. Quat. Res. 42, 188–196.
Haas, J.N., 1996. Neorhabdocoela oocytes - palaeoecological indicators found inpollen preparations from Holocene freshwater lake sediments. Rev. Palaeobot. Palynol. 91, 371–382.
Heusser, L., 1998. Direct correlation of millennial-scale changes in western North American vegetation and climate with changes in the California Current system over the past 60 kyr. Paleoceanography 13 (3), 252–262.
Heusser, L.E., 2000. Rapid oscillations in western North America vegetation and climate during oxygen isotope stage 5 inferred from pollen data from Santa Barbara Basin (Hole 893A). Palaeogeogr. Palaeoclimatol. Palaeoecol. 161, 407–421.
Hevly, R.H., 1968. Studies of the modern pollen rain in Arizona. J. Ariz. Acad. Sci. 5 (2), 116–127.
Hereford, R., 2007. Climate variation at flagstaff, Arizona, 1950 to 2007: U.S. Geological Survey Open-File Report 2007–1410 17.
Holm, R.F., Nealey, L.D., Conway, F.M., Ulrich, G.E., 1989. Mormon Lake volcanic field. In: Chapin, C.E., Zidek, J. (Eds.), Field Excursions to Volcanic Terranes in the Western United States, Volume 1: Southern Rocky Mountain Region: New Mexico Bureau of Mines and Mineral Resources Memoir, vol. 46, pp. 2–9.
IPCC, 2022. In: Pörtner, H.-O., Roberts, D.C., Tignor, M., Poloczanska, E.S., Mintenbeck, K., Alegría, A., Craig, M., Langsdorf, S., Löschke, S., Möller, V., Okem, A., Rama, B. (Eds.), Climate Change 2022: Impacts, Adaptation, and Vulnerability. Contribution of Working Group II to the Sixth Assessment Report of the Intergovernmental Panel on Climate Change. Cambridge University Press (in press).
Jacobs, B.F., 1985. Identification of pine pollen from the southwestern United States. Am. Assoc. Stratigr. Palynol. Contrib. Ser. 16, 155–168.
Jiménez-Moreno, G., Anderson, R.S., Fawcett, P.J., 2007a. Millennial-scale vegetation and climate changes of the past 225 kyr from western North America. Quat. Sci. Rev. 26, 1713–1724.
Jiménez-Moreno, G., Abdul Aziz, H., Rodríguez-Tovar, F.J., Pardo-Igúzquiza, E., Suc, J.-P., 2007b. Palynological evidence for astronomical forcing in Early Miocene lacustrine deposits from Rubielos de Mora Basin (NE Spain). Palaeogeogr. Palaeoclimatol. Palaeoecol. 252, 601–616.
Jiménez-Moreno, G., Anderson, R.S., Desprat, S., Grigg, L.D., Grimm, E.C., Heusser, L.E., et al., 2010. Millennial-scale variability during the last glacial in vegetation records from North America. Quat. Sci. Rev. 29, 2865–2881.
Jiménez-Moreno, G., Anderson, R.S., Atudorei, V., Toney, J.L., 2011. A high-resolution record of climate, vegetation, and fire in the mixed conifer forest of northern Colorado, USA. Geol. Soc. Am. Bull. 123, 240–254.
Jiménez-Moreno, G., Anderson, R.S., 2013. Pollen and macrofossil evidence of Late Pleistocene and Holocene treeline fluctuations from an alpine lake in Colorado, USA. Holocene 23 (1), 68–77.
Jiménez-Moreno, G., Anderson, R.S., Shuman, B.N., Yackulic, E., 2019. Forest and lake dynamics in response to temperature, North American monsoon and ENSO variability during the Holocene in Colorado (USA). Quat. Sci. Rev. 211, 59–72.
Jiménez-Moreno, G., Anderson, R.S., Shinker, J.J., 2021. ENSO, sun and megadroughts in SW USA during the last 11,000 years. Earth Planet Sci. Lett. 576, 117217.
Johnson, B.G., Jiménez-Moreno, G., Eppes, M.C., Diemer, J.A., Stone, J.R., 2013. A multiproxy record of postglacial climate variability from a shallowing, 12-m deep sub-alpine bog in the southeastern San Juan Mountains of Colorado, USA. Holocene 23, 1028–1038.
Karl, T.R., Melillo, J.M., Peterson, T.C., 2009. Global Climate Change Impacts in the United States. Cambridge University Press.
Kaufman, D., Anderson, R.S., Hu, F.S., Berg, E., Werner, A., 2010. Evidence for a variable and wet Younger Dryas in southern Alaska. Quat. Sci. Rev. 29, 1445–1452.
Laskar, J., et al., 2004. A long term numerical solution for the insolation quantities of the Earth. Astron. Astrophys. Nor. 428, 261–285.
Lisiecki, L.E., Raymo, M.E., 2005. A Pliocene-Pleistocene Stack of 57 Globally Distributed Benthic δ18O Records. https://doi.org/10.1029/2004PA001071.
MacDonald, G., 2010. Water, climate change, and sustainability in the southwest. PNAS 107, 21256–21262.
McCabe, K.W., 1971. Geology and Botany of Stoneman Lake Area, Coconino County, Arizona. M.S. thesis. Flagstaff, Arizona, Northern Arizona University, p. 104.
Pirnie, M., Arizona Department of Environmental Quality (ADEQ), 2000. Draft Stoneman Lake TMDL: http://legacy.azdeq.gov/environ/water/assessment/download/stoneman.pdf.
Martínez-Abarca, L.R., Lozano-García, S., Ortega-Guerrero, B., Chávez-Lara, C.M., Torres-Rodríguez, E., Caballero, M., Brown, E.T., Sosa-Nájera, S., Acosta-Noriega, C., Sandoval-Ibarra, V., 2021. Environmental changes during MIS6-3 in the Basin of Mexico: a record of fire, lake productivity history and vegetation. J. S. Am. Earth Sci. 109, 103231.
Nielsen, H., Sorensen, I., 1992. Taxonomy and stratigraphy of late-glacial *Pediastrum* taxa from Lysmosen, Denmark – a preliminary study. Rev. Palaeobot. Palynol. 74, 55–75.
Metcalfe, S.E., Barron, J.A., Davies, S.J., 2015. The Holocene history of the North American monsoon: “Known knowns” and “known unknowns” in understanding its spatial and temporal complexity. Quaternary Science Reviews 120, 1–27.
NGRIP North Greenland Ice Core Project Members, 2004. High-resolution record of Northern Hemisphere climate extending into the last interglacial period. Nature 431, 147–151.
Oster, J.L., Ibarra, D.E., Winnick, M.J., Maher, K., 2016. Steering of westerly storms over western North America at the last glacial maximum. Nat. Geosci. 8, 201–205.
Otto-Bliesner, B.L., Rosenbloom, N., Stone, E.J., McKay, N.P., Lunt, D.J., Brady, E.C., Overpeck, J.T., 2013. How warm was the last interglacial? New model–data comparisons. Phil. Trans. R. Soc. A 371, 20130097.
Past Interglacials Working Group of PAGES, 2016. Interglacials of the last 800,000 years. Rev. Geophys. 54, 162–219.
Pilles, P.J., 1996. The pueblo III period along the Mogollon Rim: the honanki, elden, and Turkey hill phases of the sinagua. In: Adler, Michael A. (Ed.), The Prehistoric Pueblo World, A.D. The University of Arizona Press, Tucson, pp. 1150–1350.
Power, M.J., Marlon, J., Ortiz, N., Bartlein, P.J., Harrison, S.P., Mayle, F.E., et al., 2008. Changes in fire regime since the Last Glacial Maximum: an assessment based on a global synthesis and analysis of charcoal data. Clim. Dynam. 30 (7–8), 887–907.
Railsback, L.B., Brook, G.A., Ellwood, B.B., Liang, F., Cheng, H., Edwards, R.L., 2015. A record of wet glacial stages and dry interglacial stages over the last 560kyr from a standing massive stalagmite in Carlsbad Cavern, New Mexico, USA. Palaeogeogr. Palaeoclimatol. Palaeoecol. 438, 256–266.
Reimer, P.J., Austin, W.E.N., Bard, E., Bayliss, A., Blackwell, P.G., Bronk Ramsey, C., Butzin, M., Cheng, H., Edwards, R.L., Friedrich, M., Grootes, P.M., Guilderson, T.P., Hajdas, I., Heaton, T.J., Hogg, A.G., Hughen, K.A., Kromer, B., Manning, S.W., Muscheler, R., Palmer, J.G., Pearson, C., van der Plicht, J., Reimer, R.W., Richards, D.A., Scott, E.M., Southon, J.R., Turney, C.S.M., Wacker, L., Adolphi, F., Büntgen, U., Capano, M., Fahrni, S.M., Fogtmann-Schulz, A., Friedrich, R., Köhler, P., Kudsk, S., Miyake, F., Olsen, J., Reinig, F., Sakamoto, M., Sookdeo, A., Talamo, S., 2020. The IntCal20 northern Hemisphere radiocarbon age calibration curve (0–55 cal kBP). Radiocarbon 62, 725–757.

Sanchez Goñi, M.S., Cacho, I., Turon, J.L., Guiot, J., Sierro, F., Peypouquet, J., et al., 2002. Synchroneity between marine and terrestrial responses to millennial scale climatic variability during the last glacial period in the Mediterranean region. Clim. Dynam. 19 (1), 95–105.
Schmidt, M.W., Hertzberg, J.E., 2011. Abrupt climate change during the last ice age. Nat. Educat. Knowledge 3 (10), 11.
Seager, R., Ting, M., Held, I., Kushnir, Y., Lu, J., Vecchi, G., Huang, H.-P., Harnik, N., Leetmaa, A., Lau, N.-C., Li, C., Velez, J., Naik, N., 2007. Model projections of an imminent transition to a more arid climate in southwestern North America. Science 316, 1181–1184.
Seager, R., Vecchi, G.A., 2010. Greenhouse warming and the 21st century hydroclimate of southwestern North America. Proc. Natl. Acad. Sci. USA 107, 21277–21282.
Shuman, B.N., Marsicek, J., 2016. The structure of Holocene climate change in midlatitude North America. Quat. Sci. Rev. 141, 38–51.
Staley, S.E., Fawcett, P.J., Anderson, R.S., Jiménez-Moreno, G., 2022. Early pleistocene-to-present paleoclimate archive for the American southwest from Stoneman Lake, Arizona, USA. Geol. Soc. Am. Bull. 134 (3/4), 791–814.
Staudenmaier Jr., M., Preston, R., Sorenson, P., 2014. National Oceanic and Atmospheric Administration (NOAA) Technical Memorandum WR-273. Climate of Flagstaff, Arizona, p. 63.
Toney, J.L., Anderson, R.S., 2006. A postglacial paleoecological record from the San Juan Mountains of Colorado USA: fire, climate and vegetation history. Holocene 16, 505–517.
Van Geel, B., 2001. Non-pollen palynomorphs. In: Smol, J.P., Birks, H.J.B., Last, W.M. (Eds.), Tracking Environmental Change Using Lake Sediments. Volume 3: Terrestrial, Algal, and Siliceous Indicators. Kluwer Academic Publishers, Dordrecht, The Netherlands, 2001.
Van Geel, B., Coope, G.R., van der Hammen, T., 1989. Palaeoecology and stratigraphy of the Lateglacial type section at Usselo (The Netherlands). Rev. Paleobotany Palynol. 60, 25–129.
Whitlock, C., Bartlein, P.J., 1997. Vegetation and climate change in northwest America during the past 125 kyr. Nature 388, 57–61.
Williams, A.P., Allen, C.D., Millar, C.I., Swetnam, T.W., Michaelsen, J., Still, C.J., Leavitt, S.W., 2013. Forest responses to increasing aridity and warmth in the southwestern United States. Proc. Natl. Acad. Sci. USA 107 (50), 21289–21294.
Woolfenden, W.B.A., 2003. 180,000-year pollen record from Owens Lake, CA: terrestrial vegetation change on orbital scales. Quat. Res. 59, 430–444.
Yin, Q., Berger, A., 2015. Interglacial analogues of the Holocene and its natural near future. Quat. Sci. Rev. 120, 28–46.
Yuan, F., Koran, M.R., Valdez, A., 2013. Late glacial and Holocene record of climatic change in the southern Rocky mountains from sediments in san luis lake, Colorado, USA. Palaeogeogr. Palaeoclimatol. Palaeoecol. 392, 146–160.